

## INTERMITTENCY STUDY OF GLOBAL SOLAR RADIATION ON REUNION ISLAND USING HILBERT-HUANG TRANSFORM

LI Qi, BESSAFI Miloud, DELAGE Olivier, CHABRIAT Jean-Pierre, LI Peng

Laboratory of Energy, Electronic and Process (LE<sup>2</sup>P),  
University of Reunion Island,  
15 Avenue Rene Cassin,  
CS 92003, 97 744 Saint-Denis Cedex 9,  
Reunion Island, France

E-mail: richie.qili@gmail.com

### ABSTRACT

The characterization of the solar radiation variability is a fundamental step before prediction and is crucial to transform an intermittent source of energy into a stable one. As solar irradiance result from a nonlinear and non-stationary process, we use a multifractal approach based on the Hilbert-Huang Transform (HHT) consisting of an empirical mode decomposition (EMD) followed by a spectral analysis. In this paper, we will briefly introduce the HHT data analysis method. Such a recent adaptive data analysis method has been applied to Reunion Island global solar radiation time series of measurements with a sampling rate of 1/60 Hz over six years. Through the EMD, daily global solar radiation data were decomposed into several intrinsic mode functions (IMF). For each IMF, we estimate the amplitude, instantaneous frequency and Hilbert spectrum for the original data. From the comparison of Hilbert Spectrum and Fourier Spectrum, we find the calculated solar radiation power spectrum follows a power law behavior close to the Kolmogorov law. The method described in this paper provides an amplitude frequency representation of the global solar radiation sequences resulting in a probability density function and a scaling coefficient. The multifractal approach allows to extract parameters connected to the multifractal properties of the global solar radiation.

### INTRODUCTION

With the rapid development of the global economy and society, requirements for renewable energy increase remarkably. Solar energy is considered as one of the most promising alternative energy resources. However, the spatial and temporal variability of solar radiation over various time scales is difficult for computing, controlling and balancing. Solar radiation shows the characteristics, nonlinear, nonstationary and intermittency in various process [1].

Intermittency is the irregular alternation of phases of apparently periodic and chaotic dynamics or different forms of chaotic dynamics (crisis-induced intermittency) [2 3]. In the area of solar radiation, Tarroja et al. give the concept of intermittency the same meaning that to the concept of fluctuation, defining the severity of the intermittency as the change in the magnitude of the total irradiation on a surface over a given time interval [4]. Thus, this meaning is agreed with the concept of variability. On the contrary, Davis et al. import the notion of intermittency from turbulence, though they analyze radiation data artificially generated from cloud data [5]. This one is the sense given to the concept of intermittency in the present work, that is, intermittency refers to the changes of the variability of daily solar radiation according to the scale considered. In this sense, intermittency and multifractality are synonym.

Intermittency and multiscaling properties have been found in many fields, such as rainfall [11], finance [9 10], turbulence [6-8 15], and geophysical fields [12 13 28].

Multiscaling intermittency is often characterized using a structure function of order  $q > 0$  as the statistical moment of the fluctuations  $\Delta X(\tau) = |X(t + \tau) - X(t)|$  [6 15]

$$\langle (\Delta X(\tau))^q \rangle \sim C_q \tau^{\zeta(q)} \quad (1)$$

where  $C_q$  is a constant and  $\zeta(q)$  is a scale invariant moment function; it is also a cumulant generating function, which is nonlinear and concave and fully characterizes the scale-invariant properties of intermittency.

For this global solar radiation study, we consider the scaling exponent  $\zeta(q)$  that characterizes the scaling behavior or measures the distance between a monofractal and multifractal

process. Indeed if  $\zeta(q)$  is linear, the considered process is monofractal, if  $\zeta(q)$  is nonlinear, the process is multifractal. Furthermore, the concavity gives information on the intermittency degree: the more concave the curve is, the more intermittent the process [6 14 28]. In this study, scaling exponents  $\zeta(q)$  is estimated through EMD and arbitrary-order Hilbert spectral analysis [15], which is an extension of Hilbert Huang Transform (HHT) [18 19].

This paper is organized as follows. Section 2 describes the global solar radiation dataset used in this study. Section 3 presents the EMD and arbitrary-order Hilbert spectral analysis methods and the multifractal intermittency properties. Section 4 is dedicated to the presentation and the discussion of the results, which are then briefly summarized in Section 5.

## NOMENCLATURE

$X(t)$	[W/m <sup>2</sup> ]	global solar radiation
$f$	[min <sup>-1</sup> ]	frequency
$\omega$	[min <sup>-1</sup> ]	instantaneous frequency
$F_s$	[min <sup>-1</sup> ]	Sampling frequency
$T_s$	[m]	Sampling time
$T$	[m]	Time scale
$A$		Amplitude
$e$		envelop
$E(f)$		Fourier spectrum
$m$		mean
$H(\omega)$		Hilbert spectrum
$h(\omega)$		Hilbert marginal spectrum
$C(t)$		IMF mode
$j$		scale index

### Special characters

$\theta(t)$	the phase
$p(\omega, A)$	probability density function
$\beta$	spectral exponent
$\zeta(q)$	Scaling exponent
$\xi(q)$	Scaling exponent in Hilbert space

## GLOBAL SOLAR RADIATION DATASET

Reunion island is a French overseas territory and the only European region in the southern hemisphere. It lies at 21°06' South and 55°32' East, which locates in the North of the tropic of Capricorn. Due to its location, solar energy is an abundant energy resource in Reunion (cf. Fig. 1). Annual sunshine is in the range of 1400–2500 h and can reach the value of 2900 h, for an altitude lower than 400 m. The monthly daily radiation reaches more than 6.5kWh/m<sup>2</sup> during the wet season in some parts of the coastal region (altitude <300 m).

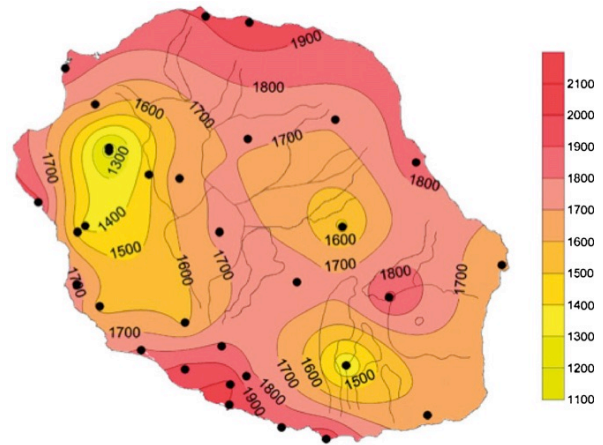


**Figure 1** Global solar irradiance (kWh/m<sup>2</sup>) distribution in Reunion [17].

In this study, we use 1234 days of global solar radiation recorded by the MOUFIA station on Reunion Island. The solar radiation measurements were collected with a sampling time  $T_s=1$  min (the sampling frequency  $F_s=1/T_s=1$  min<sup>-1</sup> = 0.01667Hz). The data time span covers 6 years, from 23 December, 2008 to 22 November, 2013, and it is presented as minutely mean. We use the time series from 8:00 to 17:00, which resulted in 661 data value for each day. During this period, the ground could obtain more solar radiation and the condition is clearer for the whole data. There are 1234\*601 data points, but these days are not all continuous.

Fig.2 a) shows our global solar radiation data from 2008 to 2013, b) illustrates a daily global solar radiation of the whole dataset. This figure shows that the solar radiations exhibit the stochastic fluctuations.

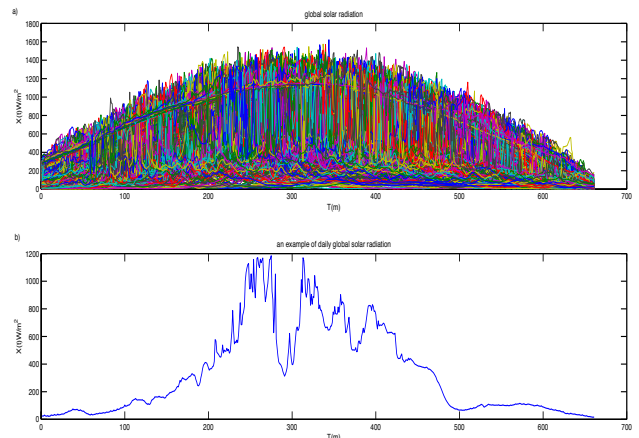


**Figure 2** a) the whole global solar radiation data, b) an example of daily global solar radiation sequence

## INTERMITTENCY AND MULTISCALING PROPERTIES: ARBITRARY ORDER HILBERT SPECTRAL ANALYSIS

We use a new method called Arbitrary Order Hilbert Spectral Analysis [12 15 28], which is the extension of Hilbert-Huang Transform [18 19], to estimate the scaling exponent  $\xi(q)$  which is the principal value of the solar radiation fluctuations.

HHT consists of two steps: 1) Empirical Mode Deposition (EMD) 2) Hilbert spectral analysis [18 19].

➤ **Empirical Mode Deposition**

EMD is used to decompose the data into a sum of different time series (modes), each one having a characteristic frequency [18-21]. The modes are called Intrinsic Mode Functions (IMFs) and satisfy the following two conditions: i) the difference between the number of local extrema and the number of zero-crossings must be zero or one; ii) the running mean value of the envelope defined by the local maximum and the envelope defined by the local minimum is zero [18 19]. The EMD procedure to decompose a signal into IMFs follows these algorithms:

- 1) The local extremes of the signal  $X(t)$  are identified.
- 2) The local maxima are connected together forming an upper envelope  $e_{max}(t)$ , which is obtained by a cubic spline interpolation. The same is done for local minima, providing a lower envelope  $e_{min}(t)$ .
- 3) The mean is defined as  $m_1(t) = (e_{max}(t) + e_{min}(t))/2$ .
- 4) The mean is subtracted from the signal, providing the local detail  $h_1(t) = X(t) - m_1(t)$ .
- 5) The component  $h_1(t)$  is then examined to check if it satisfies the conditions to be an IMF. If yes, it is considered as the first IMF and denoted  $C_1(t) = h_1(t)$ . It is subtracted from the original signal and the first residual,  $r_1(t) = X(t) - C_1(t)$  is taken as the new series in step 1). On the other hand, if  $h_1(t)$  is not an IMF, a procedure called "sifting process" is applied as many times as needed to obtain an IMF. The sifting process is the following:  $h_1(t)$  is considered as the new data; the local extrema are estimated, lower and upper envelopes are formed and their mean is denoted  $m_{11}(t)$ . This mean is subtracted from  $h_1(t)$ , providing  $h_{11}(t) = h_1(t) - m_{11}(t)$ . Then it is checked again if  $h_{11}(t)$  is an IMF. If not, the sifting process is repeated  $k$  times, until the component  $h_{1k}(t)$  satisfies the IMF conditions. Then the first IMF is  $C_1(t) = h_{1k}(t)$  and the residual  $r_1(t) = X(t) - C_1(t)$  is taken as the new series in step 1).

The above procedure is repeated for  $n$  times and such  $n$  IMFs are obtained, when  $r_1(t)$  becomes monotonic function no further IMF can be extracted. Thus the original signal  $X(t)$  is written as a sum of IMF modes  $C_i(t)$  and a residual  $r_n(t)$ .

$$X(t) = \sum_{i=1}^N C_i(t) + r_n(t). \tag{2}$$

The above sifting process should be stopped by a criterion [18-20,22,23]. This criterion has been accomplished by limiting size of the standard deviation (SD) between 0.2 and 0.3.

$$SD = \sum_0^r \left[ \frac{|d_{i-1}(t) - d_i(t)|^2}{d_{i-1}^2(t)} \right] \tag{3}$$

➤ **Hilbert spectral analysis (HSA)**

EMD is associated Hilbert spectral analysis, which is applied to each IMF component  $C_i$  as a time frequency analysis, in order to locally extract the energy-time-frequency information from the data [18 19 24 25]. The Hilbert transform is written as

$$\tilde{C}_i(t) = \frac{1}{\pi} P \int_0^\infty \frac{C_i(t')}{t - t'} dt' \tag{4}$$

where  $P$  means the Cauchy principle value [24 25]

From this, we can construct the analytic signal  $z$ , defined as

$$z = C + j\tilde{C} = A(t)e^{j\theta(t)} \tag{5}$$

where  $C$ ,  $\tilde{C}$  is real and imaginary part of a signal respectively. Where

$$A_m = |z| = \sqrt{C^2 + \tilde{C}^2} \tag{6}$$

and  $\theta(t) = \arg(z) = \arctan \frac{\tilde{C}}{C}$ .  $A(t)$  is an amplitude time series and  $\theta(t)$  is the phase of the mode oscillation [24]. Hence, the instantaneous frequency  $\omega$  is determined from the phase,

$$\omega = d\theta/dt \tag{7}$$

Within such approach and neglecting the residual, the original time series is rewritten as

$$X(t) = Re \sum_{i=1}^N A_i(t) e^{j\theta_i(t)} \tag{8}$$

where  $A_i$  and  $\theta_i$  are the amplitude and phase time series of mode  $i$  and  $Re$  means real part [18 19]. For each mode, the Hilbert spectrum is defined as the square amplitude  $H(\omega, t) = A^2(\omega, t)$ .  $H(\omega, t)$  gives a local representation of energy in the time frequency domain. Then the Hilbert marginal spectrum  $h(\omega)$  is written as

$$h(\omega) = \int_0^\infty H(\omega, t) dt \tag{9}$$

This is similar to the Fourier spectrum, since it corresponds to the energy associated to the frequency [18 19].

➤ **Intermittency and Arbitrary-order Hilbert spectral analysis**

An extension of HHT, arbitrary-order Hilbert spectral analysis was proposed by Huang et al. [12 15 28], in order to characterize the scale invariant property of signals. Here, we can define of the joint probability density function (pdf),  $p(\omega, A)$  of the instantaneous frequency  $\omega$  and the amplitude  $A$  for all the IMF modes [12 15]. Thus the corresponding Hilbert marginal spectrum is rewritten as

$$h(\omega) = \int_0^\infty p(\omega, A) A^2 dA \tag{10}$$

This expression concerns the second-order statistical moment. A generalization of this definition is considered to arbitrary-order statistical moment  $q \geq 0$  [15 28]:

$$L_q(\omega) = \int_0^\infty p(\omega, A) A^q dA \tag{11}$$

Hence, in the Hilbert space, the scale invariance is written

$$L_q(\omega) \sim \omega^{-\xi(q)} \tag{12}$$

where  $\xi(q)$  is the corresponding scaling exponent in the Hilbert space. This scaling exponent function is linked to scaling exponent function  $\zeta(q)$  of structure functions, by the expression [15 28]:

$$\zeta(q) = \xi(q) - 1 \quad (13)$$

as it is well known that  $\zeta(q) = qH$ , hence  $\xi(q) = qH + 1$ . Here  $H$  is Hurst parameter  $H = \xi(1) - 1$ . This method provides a way to estimate the scaling exponent which characterizes intermittency process.

## RESULTS

The time series [26] of global solar radiation were collected at regular intervals, and it includes information of the trend, seasonal cycle and residual. In order to make the data more stationary, we pre-process the whole global radiation data. Fig 3 illustrates that daily global solar radiation corresponding the result of preprocessing. Fig 4 exhibits this pre-processing which was applied for the whole global solar radiation data corresponding the result. In this figure, we can see the multiple fluctuations become more stationary and unseasonal. This is global solar radiation data will be used for decomposition in next step.

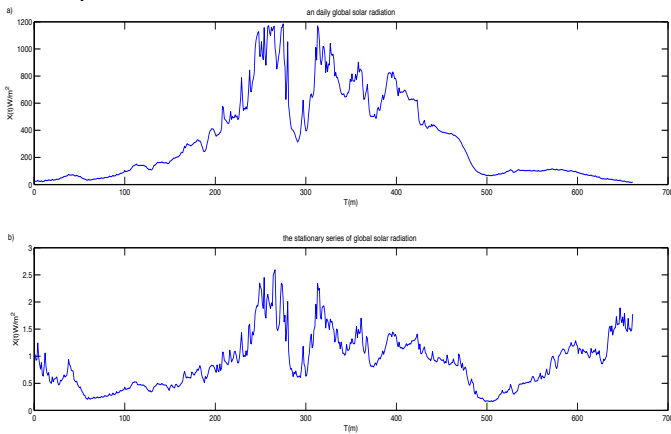


**Figure 3** An example of daily global solar radiation data and corresponding the stationary global solar radiation data.

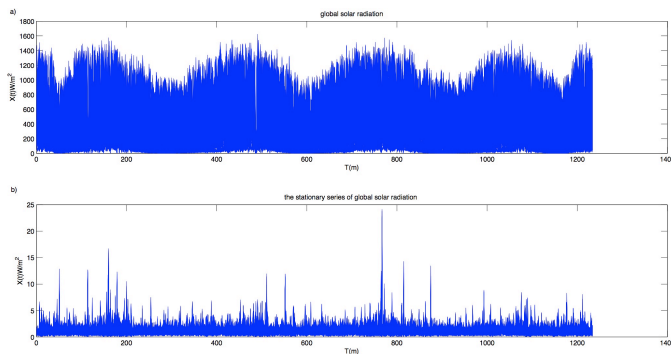


**Figure 4** The whole global solar radiation data and corresponding the stationary global solar radiation data.

### ➤ Empirical Mode Decomposition

We use EMD method to decompose the stationary daily global solar radiation data which is shown in the Fig 3. After the application of the EMD method, the original data is decomposed into IMF modes with a residual. For displaying convenience, Fig.5 illustrates the 7 IMF modes with the residual. Actually EMD acts as a filter bank to get the different time series which have a characteristic frequency. The modes (1-4) illustrate the fast fluctuations with high frequency, while the modes (5-7) represent the slower fluctuations with lower frequency. The fluctuations in these IMFs show the variability of solar radiation.

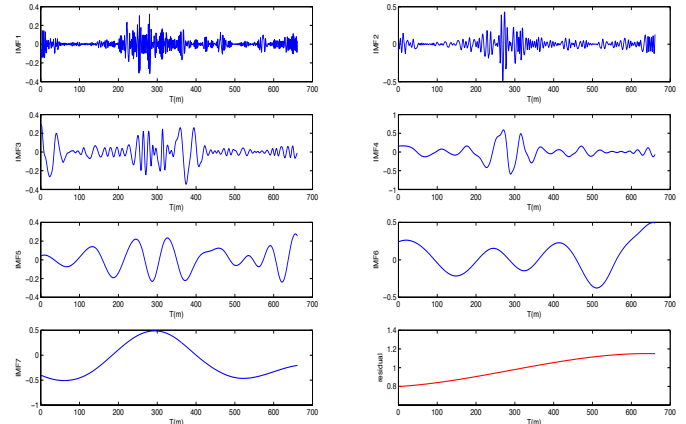


**Figure 5** IMF modes from EMD for the daily global solar radiation

### ➤ Fourier analysis and Hilbert Spectral Analysis

Fourier spectrum is used to characterize the variability of global solar radiation in this study. Fourier spectrum analysis is an important second order statistic of time-series analysis. It has long history in statistics, especially in the theory of nonparametric function and density estimation and characteristic functions [27]. For a scale invariant process, the following power law is obtained over a range of frequencies  $f$  [28]:

$$E(f) \sim f^{-\beta} \quad (14)$$

Where  $\beta$  is the spectral exponent. In Fig.6, the Fourier spectrum  $E(f)$  of the daily global solar radiation in Fig.3b was shown in log-log scale. The least square fitting method was used to estimate the slope of this Fourier spectrum, and the value of this slope is near 1.637 which is closed to the Kolmogorov spectrum with the scaling exponent  $\beta = 5/3$ , corresponding to the time scale range  $6 \text{ min} < T < 370 \text{ min}$ , corresponding the frequencies  $0.1111 \text{ min}^{-1} < f < 2.9 \cdot 10^{-3} \text{ min}^{-1}$ . We applied Fourier spectrum analysis for 1234 days solar radiation. Fig.7 illustrates the histogram of the scaling exponent  $\beta$ . The value  $\beta$  between 1.5 to 1.8 accounts 45.2%, almost 558 days. It shows that our solar radiation data displays a power law behavior.

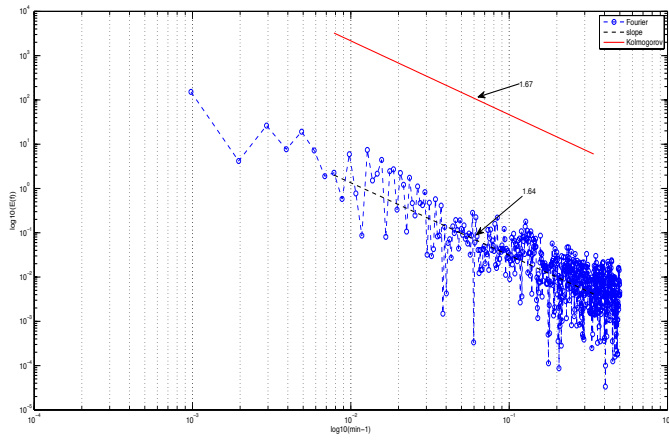


**Figure 6** The Fourier spectrum  $E(f)$  (blue line) of the solar radiation display a power law behaviour which is closed to the Kolmogorov spectrum (red line with  $\beta = -5/3$ ). The slope (black line) using least square fitting method is the scaling exponent  $\beta$  of the Fourier spectrum  $E(f)$ . The inertial frequency range is from  $0.1111 \text{ min}^{-1} < f < 2.9 \cdot 10^{-3} \text{ min}^{-1}$ .

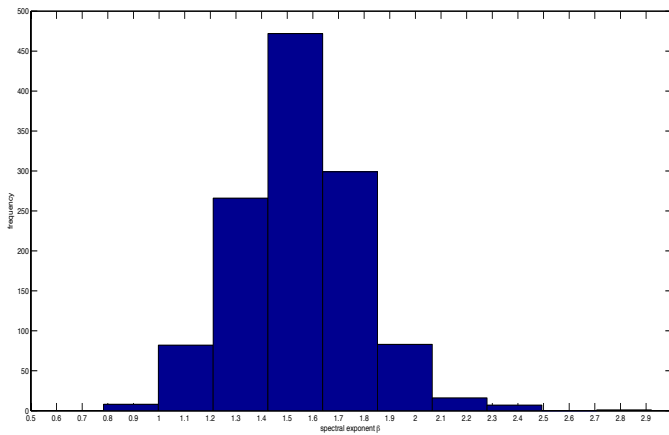


**Figure 7** The histogram of the scaling exponent  $\beta$  for the Fourier spectrum over 1234 days.

In order to characterize the intermittency of the global solar radiation, we use the IMF modes in Fig.5 to calculate the Amplitude and instantaneous frequency and apply HSA to estimate the Hilbert marginal spectrum. In the Fig.8, we compare this Hilbert marginal spectrum with the Fourier spectrum. Both of these two spectrum show a power law behaviour like  $f^\beta$  with the scaling exponent  $\beta$ . The value of  $\beta$  shows the nonlinear and non-stationary process with the increments.

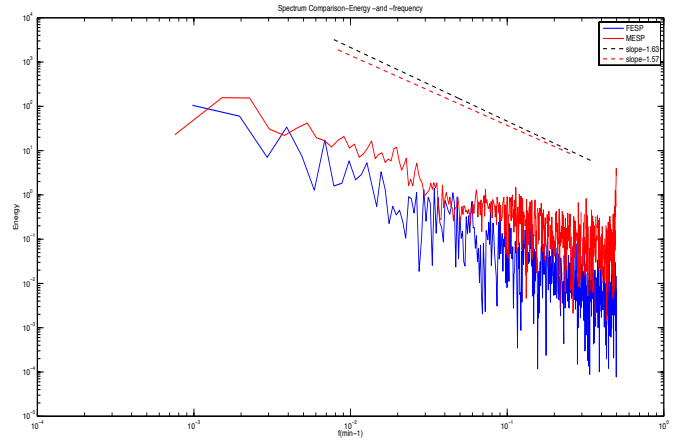


**Figure 8** The Hilbert marginal spectrum and Fourier spectrum are displayed in log-log scale. A power law behaviour closed to the Kolmogorov spectrum with the frequency inertial range  $0.1111 \text{ min}^{-1} < f < 2.9 \cdot 10^{-3} \text{ min}^{-1}$ .

### ➤ Multifractal analysis

In order to analyze the arbitrary-order moments, we estimate a representation of the joint probability density function, pdf  $p(\omega, A)$  [15] of the solar radiation. The Fig.9 illustrates that the pdf is the fluctuations in an amplitude-frequency domain over 1234 days. The pdf can't be found by one mode, and it must be obtained by all the modes together. All IMF modes of the data are calculated and then the amplitude and instantaneous frequency corresponding to each one of the IMFs could be obtained. We use these Amplitude and instantaneous frequency to estimate the pdf. In Fig.9, which shows that the amplitude varies with the variability of frequency. This pdf shows the global solar radiation the fluctuations in different frequency boundary.

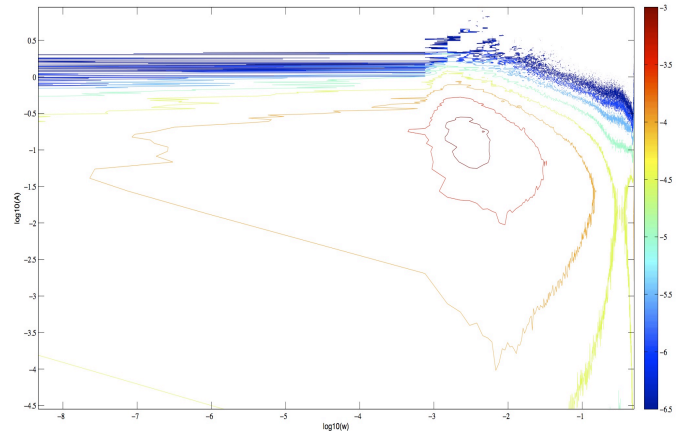


**Figure 9** The probability density function, pdf  $p(\omega, A)$  of the solar radiation.

And we also estimate the arbitrary order Hilbert marginal spectrum by using the equation 12. The Fig.10 illustrates  $L_q(\omega)$  have the variability of the intermittency where the moments  $q=0.1, 1, 2, 3$ . It show a power law behavior in range



9 min < T < 350 min corresponding the frequencies  $0.1111 \text{ min}^{-1} < f < 2.9 \cdot 10^{-3} \text{ min}^{-1}$ . The value of scaling exponent will be extracted by the least square fitting method.

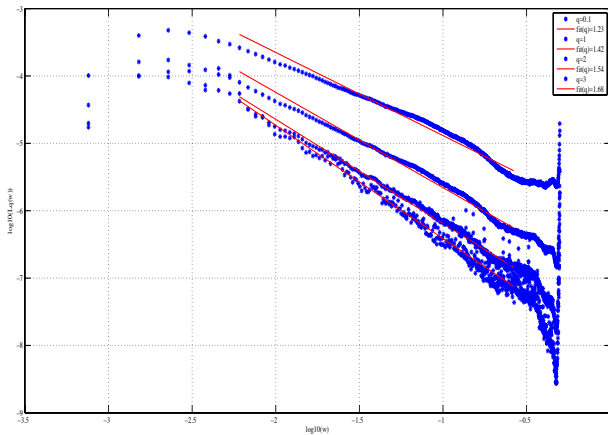


**Figure 10** Arbitrary order Hilbert marginal spectrum  $L_q(\omega)$  using different orders of moments ( $q=0.1, 1, 2, 3$ ). Power law behavior will be observed on the inertial range  $0.1111 \text{ min}^{-1} < f < 2.9 \cdot 10^{-3} \text{ min}^{-1}$  corresponding the time scales  $9 \text{ min} < T < 350 \text{ min}$ .

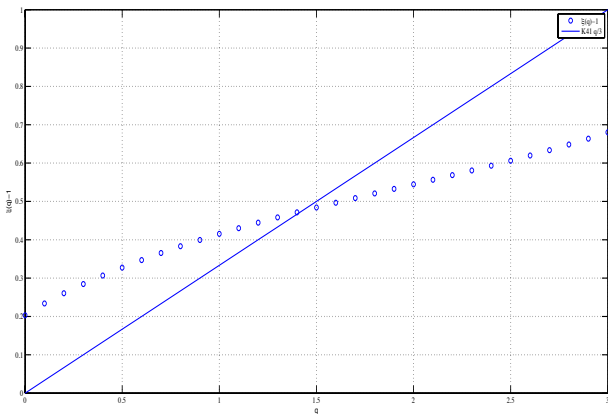


**Figure 11** Comparison of the scaling exponent  $\xi(q)-1$  with K41  $q/3$  (red line). The insert shows the difference and variability with  $q$  increments.

This provide a method to estimate the intermittency parameter  $\xi(q)$  with different order moment  $q \geq 0$ . We compare the scaling exponent  $\xi(q)-1$  with the K41 law. It seems that  $\xi(q)-1$  has departure from K41 law, and it seems less concave.

## CONCLUSION

In this paper, we applied an Empirical Mode Decomposition and Arbitrary order Hilbert spectral analysis method to characterize the intermittency of global solar radiation. The original solar radiation data (one day) is successfully separated into several IMF modes. It shows that the EMD acts as a filter bank to characterize the frequency during the time period, and it is adaptive method for decomposing the solar radiation data.

The Fourier spectrum was compared with Hilbert marginal spectrum by applying same daily solar radiation data, which turned out that the power densities related with the scaling exponent  $\beta$  which has a power law behaviour. The value of the slope is closed to  $-1.5 \sim -1.8$  over the time scale  $6 \text{ min} < T < 370 \text{ min}$ . This value range is close to the non-intermittency Kolmogorov value  $-5/3$ . It proves that the variability of solar radiation have the similar point with the turbulence over a time scale invariance.

For the whole solar radiation data (1234 days), we obtained the representation of the pdf  $p(\omega, A)$ . Using this pdf, we estimated the power densities with different order moment ( $q=0.1, 1, 2, 3$ ). Then the intermittency information was extracted out. The main advantages of this method are: 1) it seems more stable with less fluctuations for estimating the multifractal properties, 2) It provides a more adaptive schema in the time frequency analysis of solar radiation field. It is possible to apply Empirical Mode Decomposition and Arbitrary order Hilbert spectral analysis method to do more studies related on multifractal framework in the future.

## REFERENCES

- [1] Kolmogorov, A. N., A refinement of previous hypotheses concerning the local structure of turbulence in a viscous incompressible fluid at high Reynolds number, *J. Fluid Mech.*, 13, 82–85. 1962.
- [2] Mingzhou, D., Alwyn, S., ed. Intermittency, *Encyclopaedia of Nonlinear Science* (Taylor & Francis).
- [3] Edward, O., *Chaos in dynamical systems*, Cambridge University Press. p. 323. 2002.
- [4] Tarroja, B., Mueller, F., Samuelsen, S., Solar power variability and spatial diversification: implications from an electric grid load balancing perspective. *Int. J. Energy Res.* 37, 1002–1016. 2013.
- [5] Davis, A.B., Marshk, A., Cahalan, R.F., Wiscombe, W.J., Interactions: solar and laser beams in stratus clouds, fractals & multifractals in climate & remote-sensing studies. *Fractals* 5, 129–16. 1997.
- [6] Frisch, U., *Turbulence: The Legacy of AN Kolmogorov*. Cambridge University Press. 1995.
- [7] Sreenivasan, K., Antonia, R., The phenomenology of small-scale turbulence. *Annu. Rev. Fluid Mech.* 29, 435–472. 1997.
- [8] Böttcher, F., Barth, S., Peinke, J.: Small and large scale fluctuations in atmospheric wind speeds. *Stoch. Env. Res. Risk A.* 21, 299–308, 2007.
- [9] Schmitt, F.G., Schertzer, D., Lovejoy, S., Multifractal analysis of foreign exchange data. *Appl. Stoch. Models Data Anal.* 15 (1), 29–53. 1999.
- [10] Ghashghaie, S., Breymann, W., Peinke, J., Talkner, P., Dodge, Y., Turbulent cascades in foreign exchange markets. *Nature* 381 (6585), 767–770. 1996.
- [11] Schertzer, D., Lovejoy, S., Physical modelling and analysis of rain and clouds by anisotropic scaling multiplicative processes. *J. Geophys. Res.* 92 (D8), 9693–9714. 1987.
- [12] Huang, Y., Schmitt, F.G., Lu, Z., Liu, Y., Analysis of daily river flow fluctuations using empirical mode decomposition and arbitrary order Hilbert spectral analysis. *J. Hydrol.* 373, 103–111. 2009.

- [13] Mauas, P.J.D., Flamenco, E., Buccino, A.P., Solar forcing of the stream flow of a continental scale south american river. *Phys. Rev. Lett.* 101, 168501. 2008.
- [14] Schertzer, D., Lovejoy, S., Schmitt, Chigirinskaya, Y., Marsan, D., Multifractal cascade dynamics and turbulent intermittency. *Fractals* 5 (3), 427–471. 1997.
- [15] Huang, Y.X., Schmitt, F.G., Lu, Z., Liu, Y., An amplitude–frequency study of turbulent scaling intermittency using Hilbert spectral analysis. *Europhys. Lett.* 84, 40010. 2008.
- [16] INSEE Réunion. Bilan démographique 2009. Résultats no. 40; 2011.
- [17] Soler O. Atlas climatique de La Réunion. Météo France; 2000.
- [18] Hung, N.E., and al. The empirical mode decomposition and the Hilbert spectrum for nonlinear and non-stationary time series analysis, *Proc. Royal Society A-Mathematical Physical and Engineering Sciences* 454 pp. 903-995, 1998.
- [19] Huang, N.E., Shen, Z., Long, S.R., A new view of nonlinear water waves: the hilbert spectrum. *Annu. Rev. Fluid Mech.* 31 (1), 417–457. 1999.
- [20] Huang, N.E., Wu, M.L., Long, S.R., Shen, S.S.P., Qu, W., Gloersen, P., Fan, K.L., A confidence limit for the empirical mode decomposition and Hilbert spectral analysis. *Proc. R. Soc. London, Ser. A* 459 (2037), 2317–2345. 2003.
- [21] Huang, N.E., Hilbert–Huang transform and its applications. World Scientific, *Introduction to the Hilbert Huang Transform and its Related Mathematical Problems*, pp. 126 (Chapter 1). 2005.
- [22] Rilling, G., Flandrin, P., Gonçalvès, P., On empirical mode decomposition and its algorithms. In: *IEEE-EURASIP Workshop on Nonlinear Signal and Image Processing*, pp. 1–6. 2003.
- [23] Flandrin, P., Rilling, G., Gonçalvès, P., Empirical mode decomposition as a filter bank. *IEEE Signal Proc. Lett.* 11 (2), 112–114. 2004.
- [24] Cohen, L., *Time-Frequency Analysis*. Prentice Hall PTR Englewood Cliffs, NJ. 1995.
- [25] Long, S.R., Huang, N.E., Tung, C.C., Wu, M.L., Lin, R.Q., Mollo-Christensen, E., Yuan, Y., The Hilbert techniques: an alternate approach for non-steady time series analysis. *IEEE Geosci. Remote Sensing Soc. Lett.* 3, 6–11. 1995.
- [26] Brockwell P.J. and Davis, R.A., *Time Series: Theory and Methods*, Springer Series in Statistics. 1986.
- [27] Brani Vidakovic *Transforms in Statistics*
- [28] Calif, R, Schmitt, F.G. Huang, Y.X., Soubdhana, T.: Intermittency study of high frequency global solar radiation sequences under a tropical climate. *Solar Energy*, Volume 98, Part C, December 2013, Pages 349–365.